npj | vaccines

Article

Published in partnership with the Sealy Institute for Vaccine Sciences

https://doi.org/10.1038/s41541-025-01106-z

Establishing a universal IVRP method for quadrivalent HPV vaccines to replace in vivo potency tests

Jinpan Hu[1,2,7], Zijing Jia[3,7], Meng Wang[2], Lingling Nie[2], Wangjun Fu[3], Qingfeng Zhang[2], Haiyang Qin[2], Jianhui Nie[2], Xiaoyu Xu[4], Lingjie Xu[4], Fengze Wang[4], Yingping Chen[5], Bo Xing[5], Tao Li[2], Danfeng Li[6], Shaowei Li[1], Ningshao Xia[1] ✉, Xiangxi Wang[3] ✉ & Weijin Huang[1,2] ✉

Several human papillomavirus (HPV) L1-based virus-like particle (VLP) vaccines are in development to meet future global vaccination needs. Type-specific monoclonal antibodies with good reactivity to all types of vaccines are urgently needed to evaluate vaccine potency. In this study, binding activity, neutralizing activity, conformational sensitivity, immunodominance in human serum, and versatility were compared among antibodies. A broad-spectrum binding antibody (C4-F5-127) was selected as the capture antibody; four type-specific neutralizing antibodies (6-F5-77, 11-F5-187, 16-F5-196, and 18-F5-203) were selected as detection antibodies for HPV6, 11, 16, and 18, respectively. These antibodies formed a standardized and universal in vitro relative potency (IVRP) assay kit. High-resolution cryo-electron microscopy (cryo-EM) structures of HPV6-6-F5-77, HPV11-11-F5-187, HPV16-16-F5-196 and HPV18-18-F5-203 complexes define the location and nature of epitopes, revealing serotype specific binding modes and neutralization mechanisms. The IVRP results were correlated with potency data from mouse models, offering an efficient alternative to in vivo potency experiments.

According to the 2020 report by the World Health Organization's International Agency for Research on Cancer, cervical cancer has the fourth highest incidence and mortality among malignant tumors in women worldwide[1]. In the 1980s, the German scientist Harald zur Hausen discovered that human papillomavirus (HPV) infection was associated with the occurrence and development of cervical cancer; he found that high-risk HPV16 and 18 infections could cause cervical cancer and precancerous lesions in more than 70% of infected people, whereas low-risk HPV6 and 11 infections mainly caused genital warts[2,3]. L1-based HPV vaccines can prevent HPV infection, thus preventing cervical cancer[4,5]. As of December 2023, six types of HPV vaccines based on HPV virus-like particles (VLPs) were commercially available[6]. In China, more than 20 HPV vaccines are under development; these vaccines contain various VLP antigenic valences (e.g., 2, 3, 4, 9, 11, 14, and 15) and are produced in three different expression systems: yeast, *Escherichia coli*, and insect cells. However, because of factors such as research technology limitations and high production costs, the HPV vaccine supply is insufficient for current vaccination needs. The resolution of these issues and provision of widely available HPV vaccines are critical public health priorities.

The structural integrity of VLP-based vaccines is important for ensuring their potency. The structural integrity of a VLP-based vaccine can be assessed by its in vitro relative potency, which requires the measurement of type-specific antigen content[7]. When analyzing the quality of the HPV16 VLP vaccine, MERCK used an in vitro relative potency (IVRP) method that evaluated vaccine stability (i.e., batch release); the results demonstrated that data obtained using the IVRP method exhibited good consistency with data obtained from animal experiments[8]. However, few studies have investigated the correlation between in vivo and in vitro potency for HPV types other than HPV16. In China, there currently is no consensus regarding the detection antibodies, reference materials, reagents, or calculation methods

[1]National Institute of Diagnostics and Vaccine Development in Infectious Disease, School of Public Health, Xiamen University, Xiamen, 361102, China. [2]Division of HIV/AIDS and Sexually Transmitted Virus Vaccines, National Institutes for Food and Drug Control (NIFDC), No. 31 Huatuo Street, Daxing District, 102629 Beijing, China. [3]CAS Key Laboratory of Infection and Immunity, National Laboratory of Macromolecules, Institute of Biophysics, Chinese Academy of Sciences, 100101 Beijing, China. [4]Vazyme Biotech Co. Ltd, 210000 Nanjing, China. [5]Department of Immunization Program, Zhejiang Provincial Center for Disease Control and Prevention, Hangzhou, 310051, China. [6]Guangxi Institute for Drug Control, Nanning, 530021, China. [7]These authors contributed equally: Jinpan Hu, Zijing Jia. ✉e-mail: nsxia@xmu.edu.cn; xiangxi@ibp.ac.cn; huangweijin@nifdc.org.cn

used to detect type-specific antigens. The absence of consensus has led to substantial differences in detection results among studies. Although there are dozens of HPV type-specific and well characterized neutralizing monoclonal antibodies available, they may not be suitable for IVRP assays based on different expression systems, and the correlation with in vivo potency has not been well established yet, which may hinder the standardization of HPV IVRP assay methods and the use of in vitro assays to replace in vivo potency testing. The IVRP assay, which has demonstrated a robust correlation with in vivo potency, can replace the mouse model-based in vivo potency assays currently used for vaccine release detection, saving time and reducing animal use[9,10]. In accordance with the Replacement, Reduction, and Refinement (3R) and International Council for Harmonisation of Technical Requirements for Pharmaceuticals for Human Use (ICH) principles of animal welfare, H16.001 and V5 structural antibodies have been used to evaluate vaccine potency in vitro[11,12], but different antibodies are required for multivalent vaccines. Thus, there is a need to develop HPV-specific mAbs for multivalent vaccines, establish a uniform and controlled method for quantification of HPV type-specific antibodies, improve the standardization of HPV vaccine quality assessment, and promote research and development focused on high-quality HPV vaccines.

Results

Binding and neutralizing activities of an antibody panel

Human IgG1 mAbs were obtained by screening, sequencing, and recombination of single B cells isolated from vaccinated individuals. A panel of antibodies against four types of antigens (15 HPV6-specific mAbs, 11 HPV11-specific mAbs, 11 HPV16-specific mAbs, seven HPV18-specific mAbs, and eight HPV6/11/16/18-cross-binding mAbs) was established. Enzyme-linked immunosorbent assays (ELISAs) were used to detect the binding activities of HPV mAbs to HPV VLP antigens. After antibody dilution, optical density (OD) values at 450/620 nm for each concentration were entered into Prism 8 software. The four-parameter fitting model was used to calculate the half-maximal effective concentration (EC_{50}) value for each mAb; a smaller EC_{50} value revealed that the mAb had stronger antigen-binding ability. As shown in Supplementary Fig. 1a, among HPV-specific mAbs, the EC_{50} values for 6-F5-77, 11-F5-187, 16-F5-196, and 18-F5-203 were all below 20 ng/ml, indicating that these mAbs had strong antigen-binding ability and could be used to identify mAbs suitable for assessment by sandwich ELISA. Because the immunoprotective effects of preventive HPV vaccines depend on the production of neutralizing antibodies, measurements of HPV VLP binding and neutralizing activities in candidate mAbs have become important aspects of vaccine potency assessment. The pseudovirion-based neutralization assay (PBNA) is regarded as the gold standard for clinical detection of neutralizing activity in mAbs. In this study, the neutralizing activities of mAbs were detected by PBNAs, which provided reference data for mAb screening via sandwich ELISA. A smaller half-maximal inhibitory concentration (IC_{50}) value revealed that the mAb had greater neutralizing activity. As shown in Supplementary Fig. 1b, among HPV-specific mAbs, the IC_{50} values of 6-F5-77, 11-F5-187, 16-F5-196, and 18-F5-203 were all below 10 ng/ml, indicating that these mAbs had robust neutralizing activity.

Conformational sensitivity of mAbs

The integrity of key epitopes on HPV VLPs is essential for vaccine potency. To ensure that the resulting mAbs reflected conformational changes in HPV VLP antigens, thereby improving quality control, this study analyzed the conformational sensitivities of mAbs to HPV VLPs. An antibody was considered conformationally sensitive if it exhibited an OD value greater than 1.0 for intact VLPs and less than 0.1 for denatured VLPs. 6-F5-77, 11-F5-187, 16-F5-196, 18-F5-203 and C4-F5-127 were identified as conformationally sensitive antibodies (Fig. 1a, b).

Immunodominance of mAbs in human anti-HPV serum

When evaluating vaccine antigen potency in vitro, the epitope recognized by an antibody should be identical (or similar) to the epitope recognized by antibodies produced by the human body after vaccination (i.e., the dominant epitope after immunization). Because neutralizing antibody titers are low in the serum of individuals naturally infected with HPV, the present study used an HPV detection antibody to block the HPV antigen binding of clinical serum samples from 57 patients immunized with 9-valent HPV vaccine from Bowei Biotechnology administered according to their recommended three-dose vaccination schedules (months 0, 2, and 6). Serum samples were collected 12 months after the first immunization. We conducted one-way ANOVA and multiple comparisons on the blocking rate of the monoclonal antibody to screen for antibodies(6-F5-77, 11-F5-187, 16-F5-196, and 18-F5-203) with higher blocking rates for IVRP method, indicating that they recognized dominant epitopes on the surface of HPV L1 VLPs as shown in Fig. 1c–f.

Antibody pairing of double antibody sandwich ELISA

HPV6, 11, 16, and 18 cross-binding antibodies were selected as capture antibodies; HPV6, 11, 16, and 18 type-specific antibodies with high binding activity, strong neutralizing activity, conformational sensitivity, and a high blocking rate in human serum were selected as detection antibodies for horseradish peroxidase (HRP) labeling. These antibodies were paired as follows. First, 96-well plates were coated with HPV6, 11, 16, and 18 cross-binding antibodies. HPV monovalent antigen bulk without aluminum adjuvant, provided by Beijing Health Guard Biotechnology, produced in the E. coli expression system were diluted to 200 ng/ml and an HRP-labeled antibody was diluted to 1 μg/ml; next, both components were mixed with chromogenic solution and the OD value was recorded. Paired mAbs with a signal-to-noise ratio of >20 were selected for subsequent screening. As shown in Fig. 1g, C4-F5-127 exhibited good binding to 6-F5-77, 11-F5-187, 16-F5-196, and 18-F5-203; therefore, it was selected as a capture mAb.

Versatility of mAbs

Coated antibodies paired with enzyme-labeled antibodies were used to detect HPV VLP monovalent antigen bulk without aluminum adjuvant (including VLPs produced by yeast, *E. coli*, and insect cells) from seven HPV vaccine manufacturers including Ruike Biotechnology (Jiangsu, China), Bowei Biotechnology (Shanghai, China), Chengdu Institute of Biological Products (Chengdu, China), Zerun Biotechnology (Shanghai, China), Innovax Biotech Co., Ltd. (Xiamen, China), Beijing Health Guard Biotechnology (Beijing, China) and Sino Biological Inc. (Beijing, China), and EC_{50} values were calculated. Detection mAb versatilities were defined as the ratio of the maximum EC_{50} value to the minimum EC_{50} value for each manufacturer; paired mAbs with a ratio of <4 (Fig. 1h–k and Supplementary Fig. 2) were selected as candidate paired mAbs for the kit. Based on the previous screening results, the type-specific mAbs 6-F5-77, 11-F5-187, 16-F5-196, and 18-F5-203 (all exhibiting high binding activity, strong neutralizing activity, conformational sensitivity, immunodominance, and detection versatility) were selected as detection mAbs for HPV6, 11, 16, and 18, respectively.

Analytical performance of IVRP method

To verify the accuracy of the new method for determining the relative potency of HPV VLPs in vitro, we selected five initial pre-dilution concentrations of HPV VLP (i.e., 50%, 75%, 100%, 150%, and 200%), and determined their activity. Each titer was measured twice by four experimenters at different times. According to the EC_{50} values of the reference and various pre-dilution concentrations, the relative potencies of the actual measurements of different concentrations of HPV VLPs were calculated, and the results of eight experiments were reported (Supplementary Table 1). As shown in Fig. 2, the relative bias of each titer relative to the measured titer value was in the range of 30%. The geometric coefficient of variation (%) of each titer relative to the measured titer value was less than 30%. The log(abscissa) of the theoretical value of the titer was used to plot the log(ordinate) of the measured value of the titer, and the least squares method was used to perform linear regression. The correlation coefficients of the linear regression equations all exceeded 0.98. Specificity refers to the ability

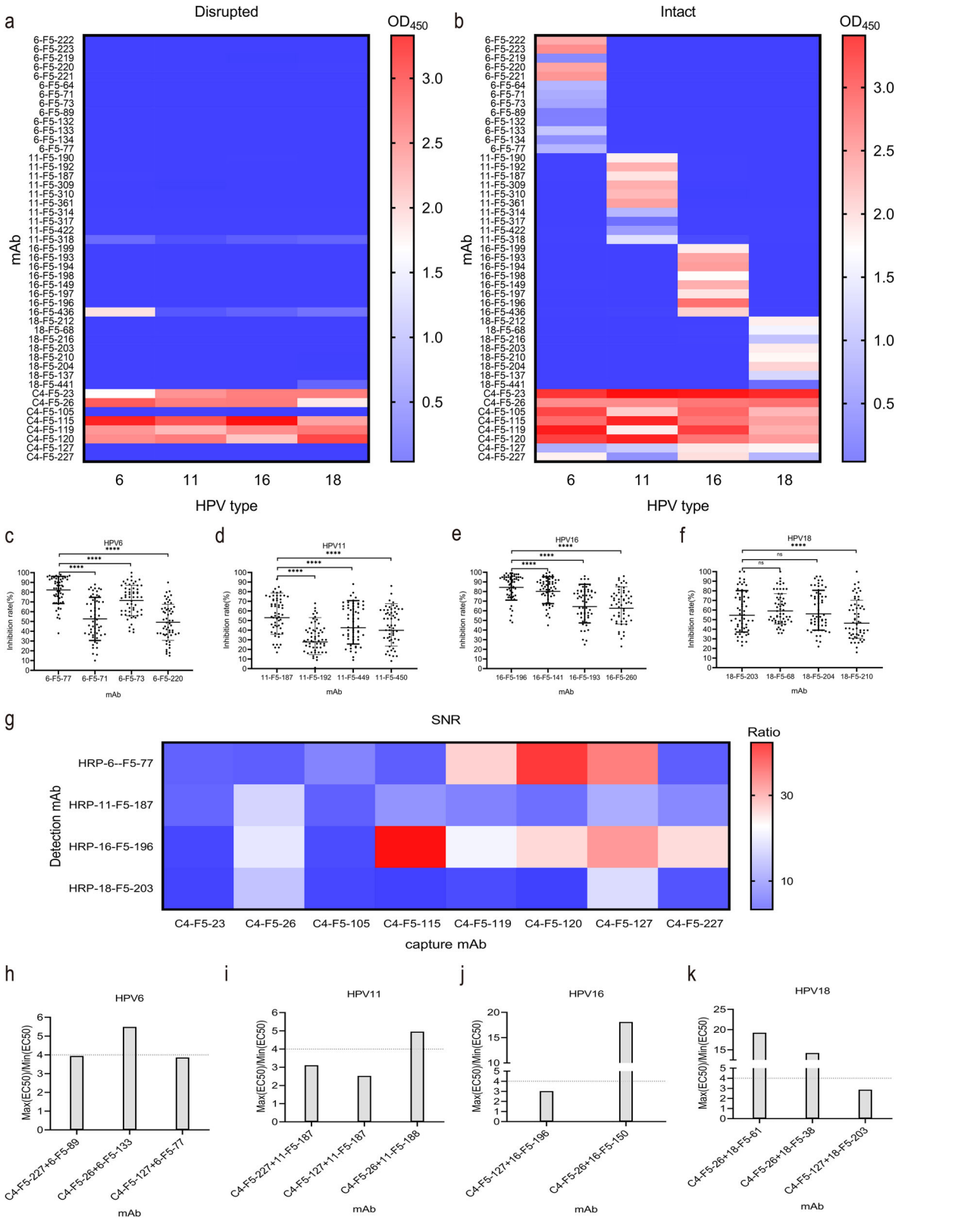

Fig. 1 | Screening of mAbs against HPV VLPs. Four types of HPV VLPs were used to coat microtiter plates as either intact VLPs (**a**, left panels) or disrupted VLPs (**b**, right panels). Inhibition ratios of the four mAbs against the 57 vaccinated human sera in HPV6 (**c**), HPV11 (**d**), HPV16 (**e**), and HPV18 (**f**). VLPs were incubated with excess amounts of human sera before the addition of competing mAb; inhibition ratios were then calculated. Each dot represents one serum sample ($n = 57$). Signal-to-noise ratio of matched mAbs in the detection of HPV VLPs, Noise refers to the absorbance value of diluent without antigen as measure in the ELISA microplate reader (**g**). The capture mAb was a type-cross-binding antibody, and the detection mAb was a type-specific antibody. Versatility of pairing for mAbs to HPV6 L1 (**h**), HPV11 L1 (**i**), HPV16 L1 (**j**), and HPV18 L1 (**k**) VLPs from seven vaccine manufacturers. The ratios of the maximum and minimum values of EC_{50} among seven vaccine manufacturers are indicated on the y-axis, and mAb pairs are indicated on the x-axis.

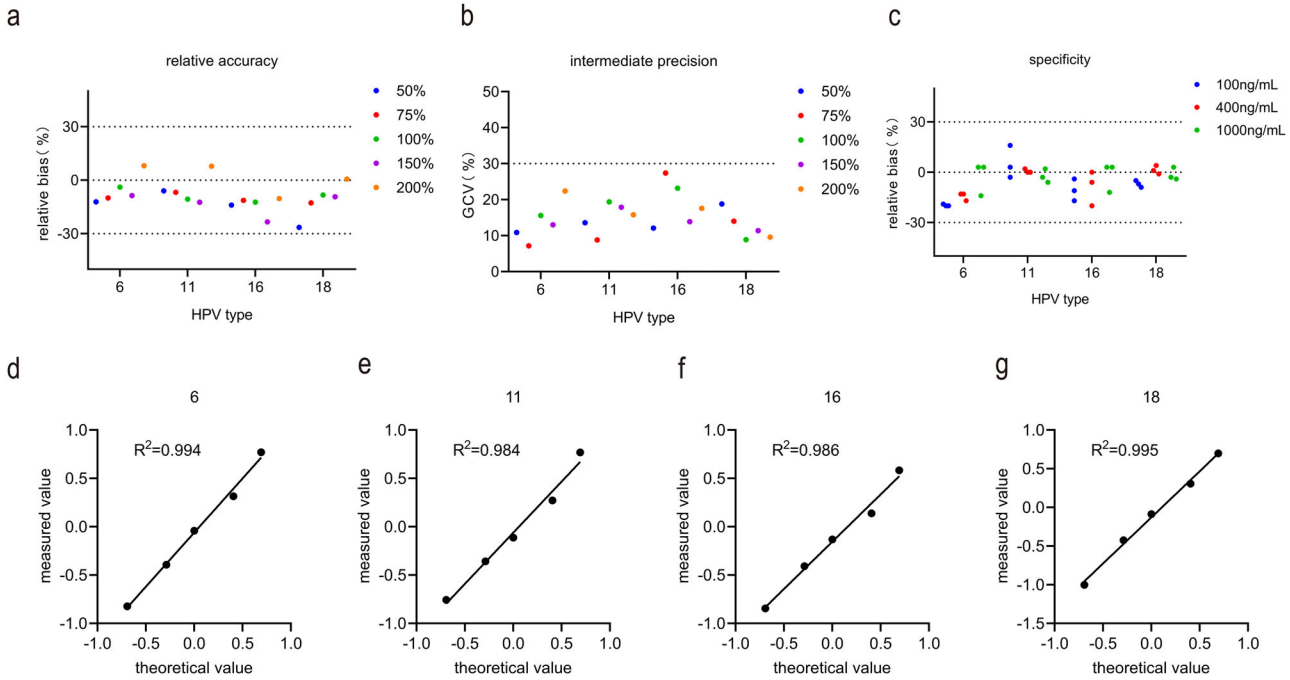

Fig. 2 | Results of relative accuracy, intermediate precision specificity, and linearity tests. a Relative accuracy refers to the degree to which the measured relative potency is close to the true value within a specified range, generally expressed as relative bias. **b** Intermediate precision refers to the geometric coefficient of variation (GCV) of relative potency measurements at each potency level. **c** specificity refers to relative bias of measured values between individual antigens and four mixed antigens at concentrations of 100, 400, and 1000 ng/ml with a ratio of 1:1:1:1. **d–g** linearity. Tests were performed by four experimenters at two different times, using five concentrations in the range of 50–200% (The concentration range of HPV6, HPV16 and HPV18 is from 10 to 40 ug/ml, The concentration range of HPV11 is from 5 to 20 ug/ml). Each point indicates the mean of eight replicates. Tests were performed using three concentrations in the range of 100 ng/ml to 1000 ng/ml.

of a measurement method to distinguish related substances. This metric was analyzed during the addition of different types of HPV antigens to a single type of test antigen (i.e., to assess the abilities of mixes containing four types of HPV antigens (6/11/16/18) and type-specific detection mAbs to detect the binding activities of the other three antigens). The four antigens were mixed at concentrations of 100, 400, and 1000 ng/ml with a ratio of 1:1:1:1. Relative bias was measured, and specificity was evaluated (values < 30% were preferred). The experiment was repeated three times.

Structures of HPV L1 pentamer and antibody complexes

To elucidate the epitopes, binding characteristics, and neutralization mechanisms of the four selected antibodies, we conducted structural analysis of the HPV L1 and antibody complexes. The high heterogeneity of HPV VLPs hinders high-resolution structural determination. Therefore, we depolymerized HPV VLPs into homogeneous and stable HPV L1 pentamers using the deoxidizing agent DTT. HPV L1 pentamer and antibody complexes were prepared by mixing HPV L1 with individual Fab fragments at a molar ratio of 1:1.2 for cryo-electron microscopy (cryo-EM) investigation. The cryo-EM structures of the 6-F5-77, 11-F5-187, 16-F5-196, and 18-F5-203 complexes were determined at resolutions of 4.3, 3.1, 2.9, and 2.9 Å, respectively (Fig. 3 and Supplementary Fig. 3). The high-quality electron density maps generated by cryo-EM allowed us to build models of these four complexes (Supplementary Fig. 4). We observed two distinct binding patterns for the four antibodies: five 16-F5-196 Fabs were clustered around one pentamer, whereas one Fab molecule was vertically bound to the central region of one L1 pentamer for the other three antibodies (Fig. 3a–d, left panels). Similar binding modes were previously reported[13,14]. In the broader context of the capsid structure, these four antibodies targeted conformational epitopes within the pentamer (Fig. 3a–d, right panels, and Supplementary Fig. 5), rather than epitopes along the edges of the pentameric blocks of the capsid. Thus, they recognized any forms of VLPs comprising various numbers of L1 pentamers from different expression systems, offering a structural explanation for the universality of these IVRP candidate antibodies. Specifically, 6-F5-77, 11-F5-187, and 18-F5-203 bound to one side of the central cavity of the pentameric plateau, where they contacted 2–3 copies of the neighboring L1 (Fig. 3a–d, right panels, and Supplementary Fig. 4). Previous studies have indicated that the minor capsid protein L2 resides within the axial cavity of the L1 pentamer and mediates HPV infection through exposure of its N terminus, which is cleaved by the proprotein convertase furin[15–17]. Therefore, these three antibodies might inhibit HPV infection by blocking conformational changes on the L1 capsid necessary for infection or by blocking L2 N-termini that protrude onto the capsid surface, subsequently preventing recognition and cleavage by furin. However, five 16-F5-196 Fabs were clustered on the top and rim of one pentamer; one Fab interacted with a copy of L1. Each pentamer can bind to 5 antibody Fabs without spatial hindrance, so this antibody can bind to VLPs to the maximum extent. Based on structural prediction, it is speculated that VLPs can theoretically bind up to 360 antibodies. This binding can occur almost on the entire surface of the HPV16 capsid and can maximize the inhibitory effect against binding to cellular receptors. Additionally, the saturated occupancy of 16-F5-196 is consistent with the experimental observation of up to 90% inhibition against vaccinated human sera.

The tight binding between HPV6 L1 and 6-F5-77 was achieved through a network of hydrophobic interactions formed by F112, G123, S124, P128, and G129 from HPV6 L1; Y33, N54, R100, Y101, and Y104 from the heavy chain; and hydrophilic interactions, including 13 hydrogen bonds. The epitope for 11-F5-187 contained 10 residues, which were primarily located in the L1 DE-loop (Y123, D124, N128, G130, Y132, G134, and N135), FG-loop (N278 and N279), and HI-loop (S354) of HPV11. Extensive hydrophilic interactions contributed to the high binding affinity between 11-F5-187 and HPV11. Similar to 6-F5-77, interactions between HPV18 L1 and 18-F5-203 consisted of a network of hydrophobic interactions formed by P121, F122, A134, V139, and M282 from HPV6 L1; F27,

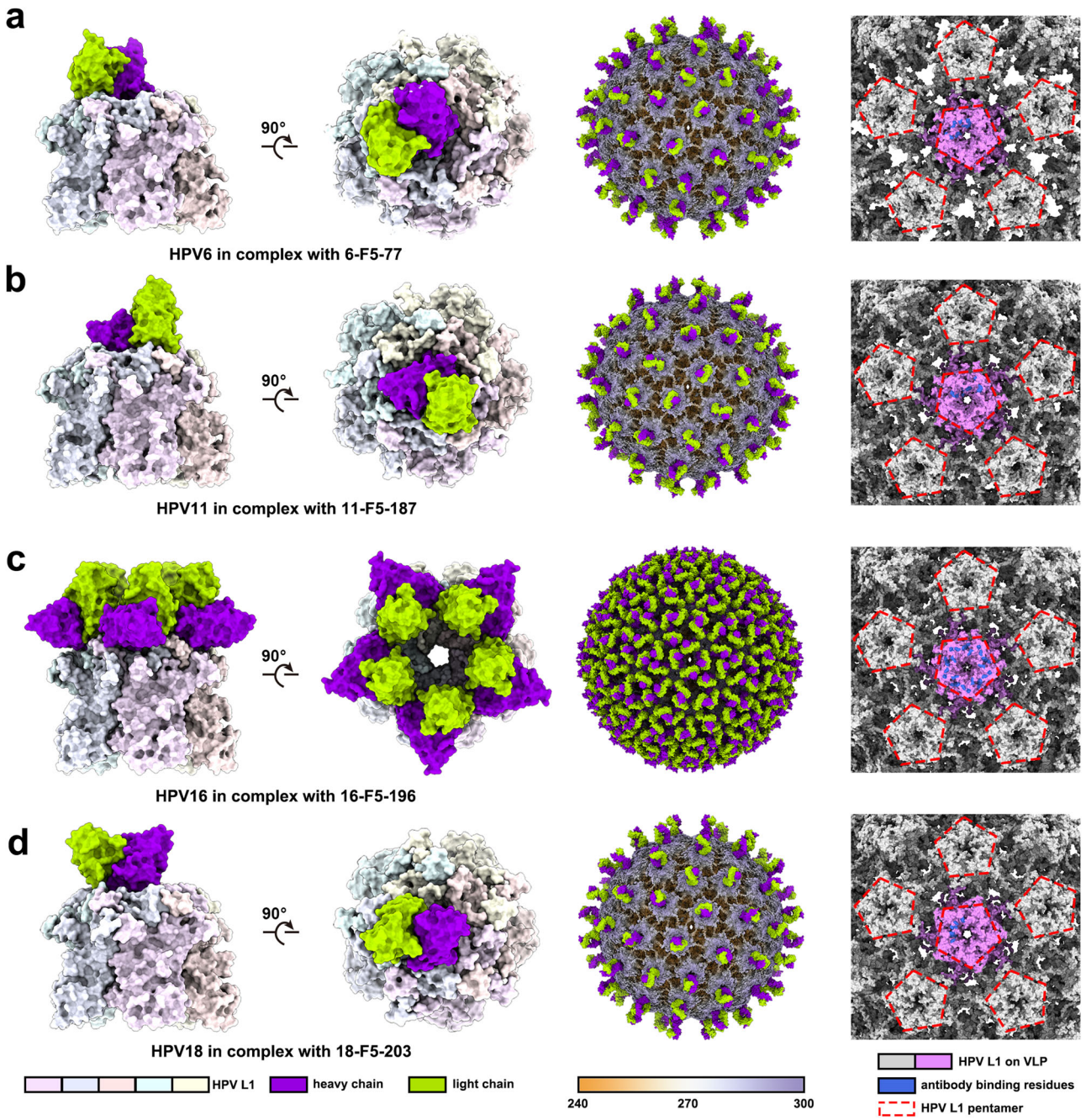

Fig. 3 | Structural basis of HPV type-specific antibodies. Side and top views (left panel) of cryo-EM maps of **a** HPV6 L1 pentamer in complex with 6-F5-77, **b** HPV11 L1 pentamer in complex with 11-F5-187, **c** HPV16 L1 pentamer in complex with 16-F5-196, and **d** HPV18 L1 pentamer in complex with 18-F5-203. Diagram (middle panel) of **a** 6-F5-77 in combination with HPV6 VLP, **b** 11-F5-187 in combination with HPV11 VLP, **c** 16-F5-196 in combination with HPV11 VLP, and **d** 18-F5-203 in combination with HPV18 VLP. Surface representing the interaction region between HPV VLPs and antibodies on HPV VLPs (right panel). Pink areas represent antibody binding sites, and dashed boxes represent HPV L1 pentamers. Bars at the bottom indicate the colors of HPV L1 and antibody.

Y35, Y50, W92, and W99 from the light chain; Y104 and I106 from the heavy chain; and hydrophilic interactions, including 11 hydrogen bonds. However, the epitope of 16-F5-196 mainly included residues N138 and A139 of the HPV16 DE-loop; residues N270, K278, S280, G281, and N285 of the HPV16 FG-loop; and residue K356 of the HPV16 HI-loop (Fig. 4a and Supplementary Table 2). The epitopes of these antibodies were mainly distributed on the HPV L1 DE, FG, and HI-loops, which are also often mapped as neutralizing epitopes[13,14]. Based on the amino acid sequence conservation analysis of 9-valent HPV types, the type-specific mAbs 6-F5-77, 11-F5-187, 16-F5-196, and 18-F5-203 primarily bound to the most variable regions of the HPV L1 DE, FG, and HI-loops (Fig. 4b and Supplementary Fig. 6). The sequence specificities of binding sites targeted by these four antibodies determine their type-specific recognition and neutralization. Furthermore, in a comparative analysis of the structural conformation of the main binding regions of the DE, FG, and HI-loops among the four specific antibodies targeting HPV L1, 6-F5-77, 16-F5-196, and 18-F5-203 predominantly bound to positions within the DE/FG-loop, which also displayed significant conformational differences. Similarly, 11-F5-187 primarily bound to a position with substantial conformational variation in the FG-loop (Fig. 4c, dashed box). Collectively, these antibodies exhibited high conformational sensitivity because they mainly interacted with regions exhibiting structural plasticity on HPV L1.

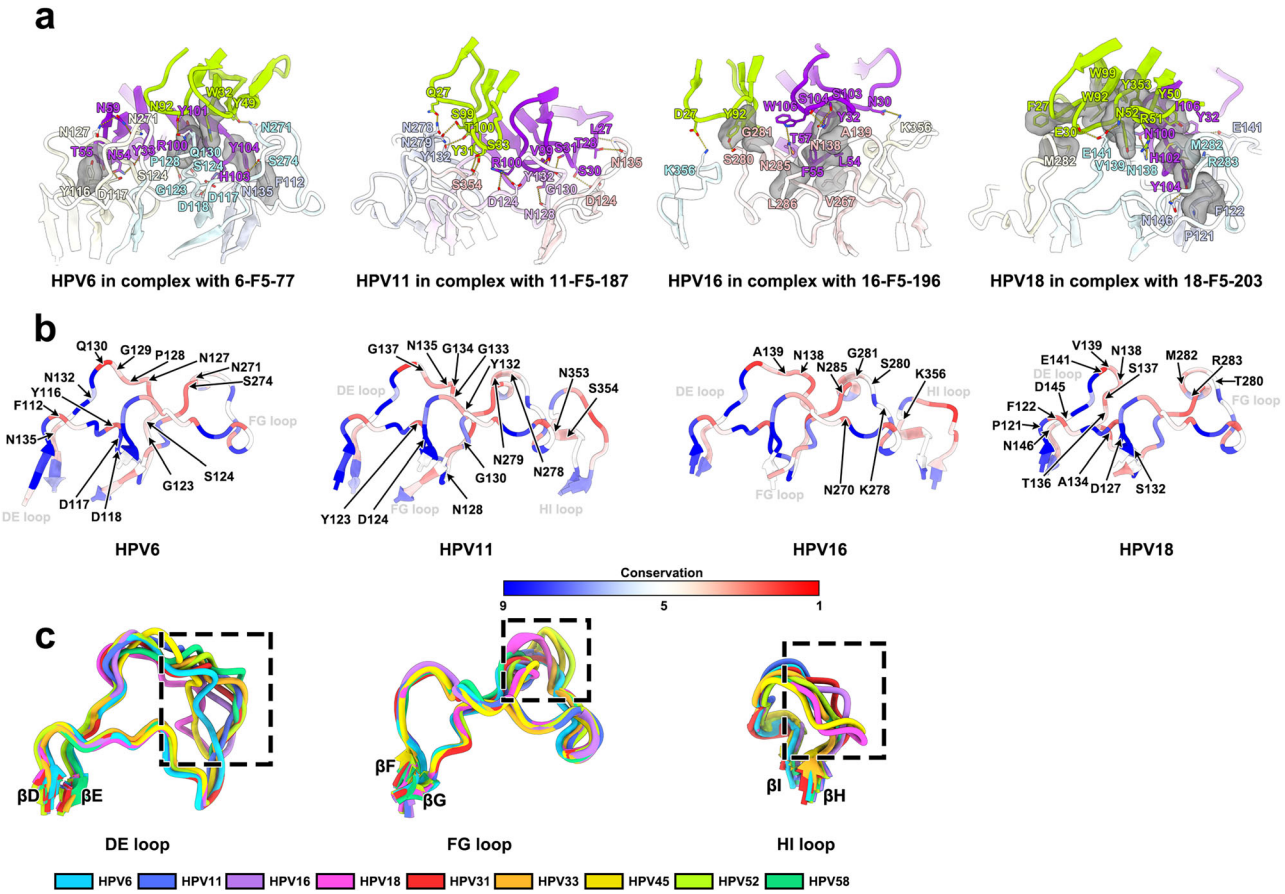

Fig. 4 | Interactions between HPV type-specific antibodies and HPV L1 loops. **a** Binding interface structures of HPV6 L1 pentamer in complex with 6-F5-77, HPV11 L1 pentamer in complex with 11-F5-187, HPV16 L1 pentamer in complex with 16-F5-196, and HPV18 L1 pentamer in complex with 18-F5-203. Color scheme is identical to Fig. 3. Yellow dashed lines represent hydrophilic interactions, and gray transparent surfaces represent hydrophobic pockets formed by hydrophobic interactions. **b** Sequence conservation analysis. The loops of HPV L1 involved in interactions between HPV L1 and type-specific antibodies (HPV DE/FG/HI loop) are aligned with the loops of other HPV 9-valent types, which are colored according to sequence conservation as listed in the table below. **c** Structure conservation analysis. The DE/FG/HI loops of HPV 9-valent types colored in the signature color scheme are superimposed on each other. Dashed boxes indicate locations with large differences in sequence structure. (The HPV6 L1 sequence was used as a reference, DE-loop: 122–128, FG-loop: 267–274, and HI-loop: 337–341).

Correlation between in vitro and in vivo potency

The in vivo potency and in vitro relative potency were measured simultaneously, including a dissolution step with citrate was performed prior to the in vitro relative potency assays. As shown in Fig. 5, after immunization with vaccines subjected to different degrees of destruction, the neutralizing antibody titers in mouse sera showed a decreasing trend for vaccines against HPV6, 11, 16, and 18; The in vitro relative potency exhibited a decreasing trend for vaccines against HPV6, 11, 16, and 18 after different degrees of destruction. Correlation analysis was performed between the in vivo potency and in vitro relative potency. As shown in Fig. 5, the correlation coefficients (R^2 values) between in vivo and in vitro potencies for vaccines against HPV6, 11, 16, and 18 were 0.89, 0.58, 0.70, and 0.96, respectively; these values were greater than 0.5, indicating a good correlation. This experiment provided strong evidence that the in vivo potency method established in this study can serve as a sensitive measure of vaccine quality. It also strongly supports the use of in vitro experiments as an alternative method that reduces the number of animals used while meeting the requirements of the 3R principle and ICH.

Collaborative validation

The four-type IVRP kits were distributed to six vaccine manufacturers for collaborative validation. The relative potencies of three batches of HPV bulk and three batches of final products were simultaneously measured using the kit and each manufacturer's in-house method including detection antibodies suitable for detecting their own VLP antigens and screened by their own companies, this experiment was repeated three times. As shown in Fig. 6, the in vitro relative potency test results of three batches of monovalent antigens and three batches of finished vaccines from six HPV manufacturers were all between 0.5 and 2.0; they were primarily concentrated around 1.0, approximating a normal distribution and indicating that the kit can be used to detect both vaccine stock solution and finished products. Comparison of the in vitro relative potency test results between the kit method and the manufacturers' methods revealed that the biases of Lab1, Lab2, Lab3, Lab4, Lab5, and Lab6 in the three batches of stock solution from each manufacturer were acceptable at < 50%. These findings revealed that the test results for the three batches with relative bias > 50% considerably varied

Discussion

In this study, analyses of binding activity, neutralizing activity, conformational sensitivity, immunoreactivity, and universality of the HPV6, 11, 16, and 18 mAbs revealed five representative mAbs. A double antibody sandwich ELISA method was established and validated for universal IVRP assessment. The developed method could identify HPV stock solution and completed vaccines for the corresponding HPV subtypes from multiple manufacturers. Furthermore, the method showed robust universality, and its detection results were similar to the results of in-house methods. When HPV VLPs were denatured by treatment with 56 °C heat or DTT, the measured values significantly decreased, indicating that this method could be used to monitor antigenic drift during production. Neutralization of these antibodies implies neutralization of their epitopes. We observed two distinct binding patterns for

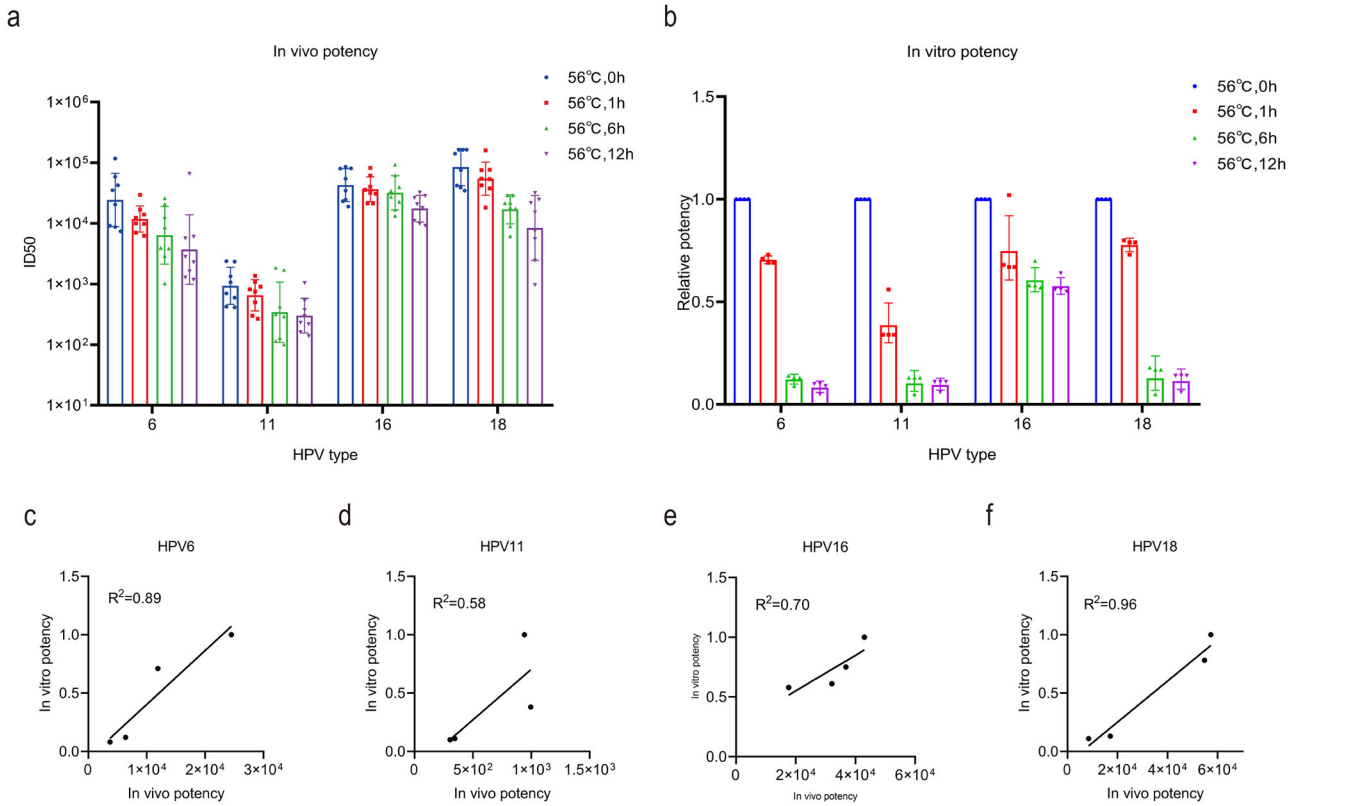

Fig. 5 | Correlations between in vivo potency and in vitro potency results for Gardasil vaccine samples containing HPV6, 11, 16, and 18 VLPs. a In vivo potency was tested by PBNA. Each column represents the mean of eight mice. **b** In vitro potency was tested by ELISA. Each column represents the mean of four replicates. The results plotted are from samples subjected to 56 °C heat-accelerated destruction for different intervals: 0 h, 1 h, 6 h and 12 h. Comparisons of HPV6 (**c**), 11 (**d**), 16 (**e**), and 18 (**f**) were conducted using the calculated coefficient of correlation, and statistical analyses were performed using GraphPad Prism 8.

these four antibodies: five 16-F5-196 Fabs were clustered around one pentamer, whereas one Fab molecule was vertically bound to the central region of one L1 pentamer for the other three antibodies (Fig. 3a–d left panel). In the broader context of the capsid structure, these four antibodies targeted conformational epitopes within the pentamer (Fig. 3a–d, right panels, and Supplementary Fig. 5), rather than epitopes along the edges of the pentameric blocks of the capsid. Thus, they recognized any forms of VLPs comprising various numbers of L1 pentamers from different expression systems, offering a structural explanation for the universality of these IVRP candidate antibodies. Epitope-based structural studies are also necessary to fulfill ICH requirements for methods to replace in vivo experiments. The discovery of these neutralizing epitopes may also serve as a reference for vaccine design. When VLPs were incubated under mild conditions (10 mM Na_2HPO4 buffer pH 8.0 with 1 mM DTT) at 4 °C overnight, the pentamer structure remained intact, and the antigen-antibody complex structure could be observed via cryo-electron microscopy. When VLPs were incubated under harsh conditions (0.2 M sodium carbonate buffer pH 10.6 with 10 mM DTT) and dried on the plates overnight at 37 °C, our results showed that the absorbance value of ELISA significantly decreased. Therefore, we inferred that harsh denaturing conditions may disrupt the pentamer.

Concerning commercially available HPV VLP vaccines, MERCK Company reported a good correlation between HPV16 IVRP and in vivo animal experiments based on extensive experimental data, then conducted release experiments for the HPV vaccine[8]. In the present study, Gardasil was subjected to assessments of in vivo potency and in vitro relative potency after exposure to four different degrees of heat-accelerated destruction. We found that the correlation study between mouse potency and IVRP should pay attention to selecting appropriate antigen immunizing dose in mice. When the immunizing dose was 2 μg/mouse, the correlation coefficients (R^2 values) between in vivo and in vitro potencies for vaccines against HPV6, 11, 16, and 18 were 0.89, 0.26, 0.70, and 0.96, respectively. However, When the immunizing dose was 0.66 μg/mouse, the correlation coefficients (R^2 values) between in vivo and in vitro potencies for vaccines against HPV6, 11, 16, and 18 were 0.81, 0.58, 0.72, and 0.91, respectively. In summary, compared with the in vivo potency test, IVRP exhibits high efficiency, good sensitivity, a short testing interval, high repeatability, and easy operation. Therefore, IVRP is expected to gradually replace in vivo potency tests and may play an important role in the life cycle management of HPV VLP vaccines.

Among the six vaccines currently on the market, two are quadrivalent and three are bivalent. Although our method was established on the basis of a quadrivalent vaccine, it can also be applied to bivalent vaccines. Furthermore, our method was validated with products from multiple manufacturers, covering all expression systems currently used to produce recombinant protein HPV vaccines. Generally, manufacturers specify a relative potency range of 0.5–2 for product release. The general IVRP method established in this study was within the relative potency range of 0.5–2 for manufacturers that participated in collaborative validation. The mean relative potencies of HPV6, 11, 16, and 18 were 1.03, 1.08, 1.07, and 0.97, respectively. Thus, the IVRP kit developed in this study can be used by all manufacturers as a replacement for their in-house methods. In the future, other subtype detection methods can be established using our methodology, which is suitable for the evaluation of 9-valent (or greater) HPV vaccines. These additional methods may facilitate the accumulation of in vitro and in vivo research data. Our findings provide a robust in vitro method that can ultimately replace in vivo methodologies.

Methods

Plasmids, HPV bulk, HPV final products, and HPV pentamers

HPV L1/L2-expressing plasmids (p16LLw[18], p18LLw[19], p6LLw2[20], and p11Lw[21]) and the red fluorescent protein reporter plasmid pRwB[22] were

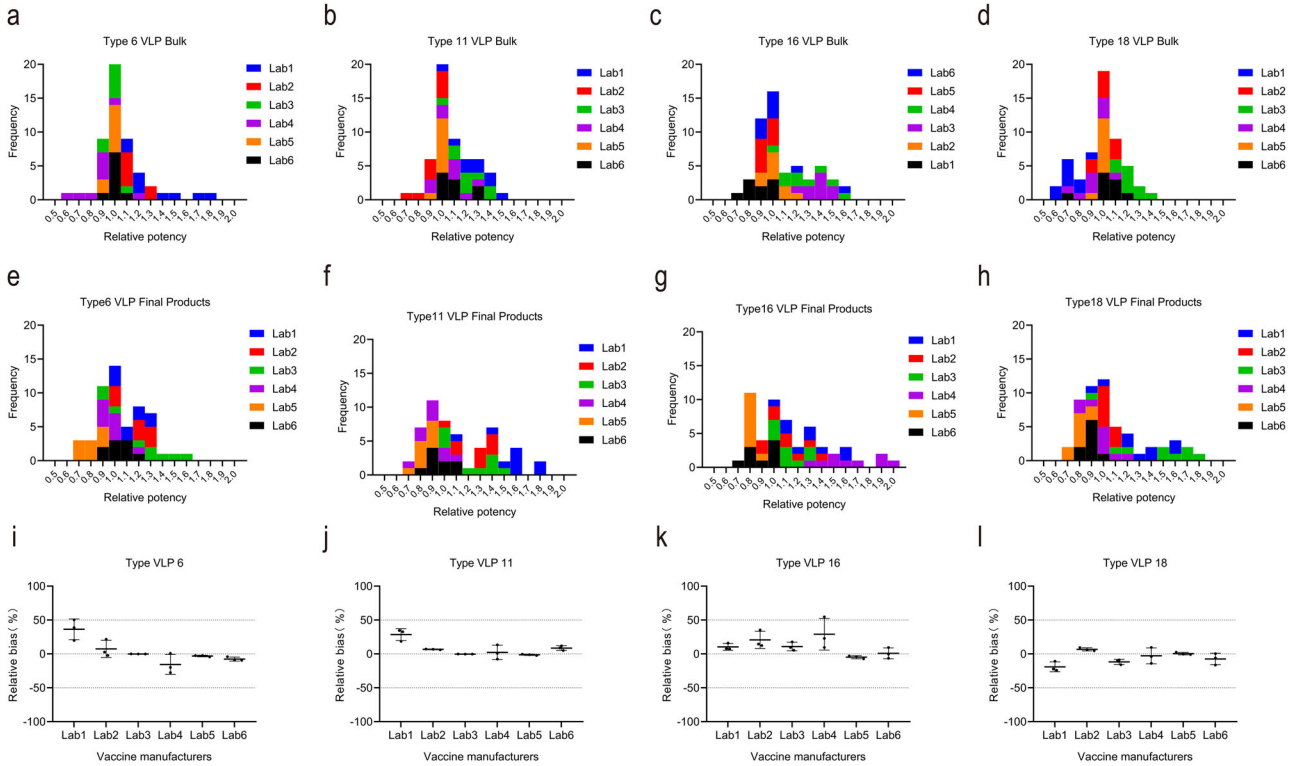

Fig. 6 | Results of collaborative validation of kits by six HPV vaccine manufacturers. a HPV6 VLP bulk, **b** HPV11 VLP bulk, **c** HPV16 VLP bulk, and **d** HPV18 VLP bulk test results from six vaccine manufacturers using the kits. **e** HPV6 VLP final product, **f** HPV11 VLP final product, **g** HPV16 VLP final product, and **h** HPV18 VLP final product test results from six vaccine manufacturers using the kits. Relative biases of **i** HPV6 VLP, **j** HPV11 VLP, **k** HPV16 VLP, and **l** HPV18 VLP test results between HPV vaccine manufacturer methods and the kit method. Three batches of VLPs were tested (in triplicate for each sample on each day) by six HPV vaccine manufacturers on three different days.

kindly provided by John Schiller (National Cancer Institute, Bethesda, MD, USA). The 293FT cell line (Invitrogen, Carlsbad, CA, USA) was maintained in growth medium (high-glucose Dulbecco's modified Eagle's medium [DMEM] with 10% fetal bovine serum [FBS], 1% penicillin-streptomycin solution, and 1% nonessential amino acids). Additionally, in the Fig. 1a–g, i–k, and Supplementary Fig. 1, HPV6, 11, 16, and 18 monovalent antigen bulk without aluminum adjuvant were kindly provided by Beijing Health Guard Biotechnology, produced in the *E. coli* expression system. In the Fig. 1h and Supplementary Fig. 2, seven types of HPV6, 11, 16, and 18 monovalent antigen bulk without aluminum adjuvant were kindly provided by the aftermentioned vaccine manufacturers. The yeast expression system was used by Ruike Biotechnology (Jiangsu, China), Bowei Biotechnology (Shanghai, China), Chengdu Institute of Biological Products (Chengdu, China), and Zerun Biotechnology (Shanghai, China). The *E. coli* expression system was used by Innovax Biotech Co., Ltd. (Xiamen, China) and Beijing Health Guard Biotechnology (Beijing, China). The insect cell expression system was used by Sino Biological Inc. (Beijing, China). As shown in the Fig. 6, VLP bulk without aluminum adjuvant and HPV final products adsorbed on aluminum adjuvant were provided by the aftermentioned vaccine manufacturers (Ruike Biotechnology, Bowei Biotechnology, Zerun Biotechnology, Innovax Biotechnology, Health Guard Biotechnology and Sino Biological Inc). The VLPs used to generate the pentamers were provided by Beijing Health Guard Biotechnology, produced in the E. coli expression system. The quadrivalent HPV vaccine adsorbed on aluminum adjuvant, Gardasil, was provided by MERCK and produced in the yeast expression system.

Single memory B cell isolation and sequencing

Peripheral blood mononuclear cells (PBMCs) were isolated from the whole-blood samples obtained from Gardasil-vaccinated individuals, administered according to recommended three-dose vaccination schedules (months 0, 2, and 6). Serum samples were collected 7 months after the first immunization (The protocol was approved by the Ethics Committee of Peking Union Medical College Hospital and the ethical approval number was ZS-2856). The samples were separated using Ficoll (Cytiva) gradient centrifugation. After washing with Hank's balanced salt solution (HBSS) (Solarbio) for three times, the cells were aliquoted and stored in liquid nitrogen in the presence of FBS and DMSO. For single memory B cell sorting, stored PBMCs were thawed and incubated with CD19 MicroBeads (Miltenyi Biotec) to screen out CD19+ B lymphocytes, which were then incubated with anti-CD3-PECy7(BD Biosciences), anti-CD27-APC (BD Biosciences), anti-IgG-PE (BD Biosciences), anti-IgM-PECy7(BD Biosciences) and 488-labeled HPV antigen proteins. The single memory B cells (CD27+, IgG+, IgM– and antigen+) were selected by flow sorting techniques and followed by sequencing and cloning.

Antibody expression and Fab generation

On the basis of the rapid amplification of cDNA ends (RACE) technique, first-strand cDNA was synthesized by reverse transcription using mRNA as the template; second-strand amplification was conducted using this template. Next, an overlapping polymerase chain reaction step was performed using double-stranded cDNA as the template, along with specific primers targeting upstream and downstream of the antibody light and heavy chain variable regions to amplify those variable regions. Nineteen mAbs were obtained by inserting the amplified light and heavy chain variable regions into the expression vector containing the conserved region of the antibody; subsequently, the antibodies were expressed in vitro[23]. The purified monoclonal antibodies 6-F5-77, 11-F5-187, 16-F5-196 and 18-F5-203 were then processed to obtain their Fab fragments using the Pierce Fab preparation kit (Thermo Scientific). In brief, the monoclonal antibody samples were first applied to desalination columns to remove the salt. Then the flow-throughs were collected and incubated with papain that was attached with

beads to cleave Fab fragments from the whole antibodies for 4 h at 37 °C. After that, the mixtures were transferred into protein A columns and the flow-throughs, the Fab fragments were collected and dialyzed into PBS buffer.

Determination of antibody binding activities

For antigen coating, HPV VLP proteins were diluted to 2 μg/ml with phosphate-buffered saline (PBS); aliquots of 100 μl per well were added to 96-well plates and incubated overnight at 4 °C. Antigen-coated plates were washed three times with 300 μl of PBS + 0.05% Tween 20 (PBST); 300 μl of 2% bovine serum albumin were added to each well for sealing, and the plates were incubated at room temperature for 2 h. Sealed plates were washed three times with PBST. Each antibody was diluted to 2 μg/ml with PBS, then serially diluted using a 2× gradient; aliquots of 100 μl were added to each well of an ELISA plate and the plate was incubated at 37 °C for 30 min. After three additional washes with PBST, secondary antibody (HRP-labeled rabbit anti-human IgG; diluted 1:5000; 100 μl/well) was added and the plate was incubated at 37 °C for 30 min. After the plate had been washed with PBST five times, 100 μl of tetramethylbenzidine color solution were added to each well and incubated at room temperature for 15 min in the dark. The reaction was terminated by adding 50 μl of 2 M H_2SO_4 solution, and the OD of each well at 450/620 nm was determined using a microplate reader.

Screening ELISA for conformation dependent binding

96-well plates were coated with VLP antigens of different HPV types under intact or disrupted conditions, provided by Beijing Health Guard Biotechnology, produced in the *E. coli* expression system. Intact VLPs for types 6, 11, 16 and 18 were solubilized in 50 mM histidine, 0.5 M NaCl, pH 6.2, and incubated overnight at 2–8 °C. VLPs were disrupted by incubation in 0.2 M sodium carbonate buffer, pH10.6, with 10 mM dithiothreitol (DTT) and dried on the plates overnight at 37 °C[24]. The diluted antibodies were incubated on blocked plates for 2 h at room temperature. The plates were washed, and HRP-conjugated goat anti-mouse IgG was added and incubated for 1 h at room temperature. Plates were washed and developed with TMB. The reaction was stopped with 2.0 N H_2SO4, and the optical density at 450 nm was read. Background wells contained only the conjugate and no mAb.

Detection of pseudovirus neutralization

The neutralizing activities of mAbs and serum were determined using a published method[19,25–27]. Briefly, a 384-well plate was used; the edges were sealed by adding 70 μl of sterilized water to the peripheral pores. B2-O2 was added to 20 μl of DMEM-based complete medium (1% double antibody, 1% L-glutamine, 1% nonessential amino acid, and 10% FBS), and B23-O23 was added to 10 μl of DMEM-based complete medium. Test samples were added to a 96-well U-shaped plate at an initial dilution of 40×, then serially diluted fourfold, yielding seven gradients in total. The contents of two 96-well U-shaped plates were transferred to corresponding 384-well cell culture plates; the contents of one well in a 96-well plate were transferred to two wells in a 384-well plate (10 μl/well). Pseudovirus was diluted to 200 dots per well using DMEM-based complete medium, and aliquots of 10 μl/well were added to the cell culture plates. The cell culture plates were centrifuged at 106 g for 20 s. After trypsin digestion, 293FT cells were counted. The digested cells were diluted 10-fold and added to cell counting plates. The cell concentration was adjusted to 1.5×10^5 cells/ml, and aliquots of 20 μl/well were added to the cell culture plates. The final number of cells per well was 3×10^3. After cells had been added, the cell culture plates were centrifuged at 106 g for 20 s. Fluorescence spots were detected and counted using an ELISPOT plate reader. The infection inhibition rate was calculated using the following formula: Infection inhibition rate (%) = 1 − (sample detection value − cell control value)/(virus control value − cell control value) × 100%. ID_{50} and IC_{50} were calculated by the Reed–Muench method[28].

Antibody competition assay

Based on the experience of MERCK's 9vHPV cLIA method established on the Luminex 200 instrument platform,microsphere coupling was performed[29,30]. Briefly, for four types of magnetic fluorescence carboxyl microspheres,100 μl (1×10^7/mL, NovaStar, NZK biotech, hubei, China) of each was used. For antigen and microspheres conjugation, carboxyl groups were activated in MES buffer, and then 5 μg of specific VLP antigens were conjugated to a microsphere. Four VLP microspheres were preparated. After dilution, the microsphere concentration was determined to be 1×10^6/mL using NovaHT system (NZK biotech, hubei, China) and stored in pH 7.4 PBS buffer containing 20 mM histidine. The cLIA biotinylated antibodies that are specific to dominant neutralizing epitopes. Brifly, sufficient volume of 10 mM NHS-LC-Biotin was added in pH6.5 PBS buffer at 4 °C for 24 h. For the experiment, firstly, vaccine-immunized human serum was diluted 50-fold, then added 50 μl to the reaction system with 50 μl mixed microspheres(2×10^3 of each microsphere in ph7.4 PBS containing 20 mM histidine)and incubated at 37 °C for 60 min (The protocol was approved by the Ethics Committee of Zhejiang Provincial Center for Disease Control and Prevention and the ethical approval number was T-043-R). After incubation, the microspheres were magnetically attracted and washed once with PBST for 1 min. Then the antibody was diluted to 200 ng/ml, and mixed with four coated microspheres in a 96-well plate (50 μl/well) followed by a PBST wash. Then, the supernatant was removed,SA-PE (NZK biotech,hubei,China) solution at 167 ng/mL was added and incubated at 37 °C for 20 min. Magnetically attracted microspheres without supernatant were resuspend in PBS buffer, and NovaHT systerm were used to collect signals from microspheres and SA-PE. Finally, SA-PE signals from each type of microsphere were analyzed using a computer with Microsoft Excel. The SA-PE signals were compared between reaction groups with and without serum, and the blocking rate was calculated using the following equation: blocking rate (%) = (serum group/blank group − 1) × 100%.

Validation of IVRP methodology

Validation of the IVRP methodology was conducted with reference to the Guiding Principles for Verification of Activity/Titer Determination Methods of Biological Products 9401 in Part III of the Chinese Pharmacopoeia 2020. Using HPV6 as an example, an HPV6 VLP stock solution was diluted to 20 μg/ml for the reference solution and 10, 15, 20, 30 and 40 μg/ml for the test solutions. Then, reference and test solutions were diluted threefold in 96-well plates (eight dilutions in total), and each dilution was tested in two wells. Accordingly, the theoretical relative titers of the five solutions to be tested were 50%, 75%, 100%, 150%, and 200%, respectively. Each titer was measured twice by four experimenters at different times, and the results of eight experiments were reported.

Cryo-EM sample preparation and data collection

HPV6, 11, 16, and 18 L1 pentamers, provided by Beijing Health Guard Biotechnology, produced in the *E. coli* expression system, were separately mixed with each of the Fab fragments of 6-F5-77, 11-F5-187, 16-F5-196, or 18-F5-203 at a molar ratio of 1:1.2 and incubated at 4 °C for 30 min. Aliquots (3 μl) of the complexes were deposited onto pre-glow-discharged holey carbon-coated gold grids (C-flat, 300-mesh, 1.2/1.3, Protochips Inc.), blotted for 6 s without force in 100% humidity, and immediately immersed in liquid ethane using a Vitrobot (FEI). Cryo-EM datasets of these complexes were collected at 300 kV with an FEI Titan Krios microscope (FEI). Movies (32 frames, each 0.2 s; total dose, 50 $e^-/Å^2$) were recorded using a K3 Summit direct detector with a defocus range of 1.2–1.8 μm. Automated single particle data acquisition was conducted using SerialEM software, with a calibrated magnification of 22,500 yielding a final pixel size of 1.07 Å.

Cryo-EM data processing

In total, 2867, 4022, 4009, and 3145 micrographs of the HPV6 L1-6-F5-77 complex, HPV11 L1-11-F5-187 complex, HPV16 L1-16-F5-196 complex, and HPV18 L1-18-F5-203 complex, respectively, were recorded and subjected to beam-induced motion correction using motionCorr in the Relion 3.0 package[31]. For each micrograph, the contrast transfer function was estimated using Gctf software[32]. Then, 402,464, 7,052,664, 1,819,608, and 342,630 particles of the HPV6 L1-6-F5-77, HPV11 L1-11-F5-187, HPV16

L1-16-F5-196, and HPV18 L1-18-F5-203 complexes, respectively, were picked and extracted for reference-free two-dimensional classification and three-dimensional classification by cryoSPARC software[33]; no symmetry was imposed when producing potential conformations for the complexes. Next, the candidate model for each complex was selected and processed by non-uniform auto-refinement and postprocessing in cryoSPARC to generate the final cryo-EM densities for HPV6 L1-6-F5-77, HPV11 L1-11-F5-187, HPV16 L1-16-F5-196, and HPV18 L1-18-F5-203 complexes. Resolution of the interface between L1 pentamers and mAbs was improved by performing block-based reconstruction to obtain the final resolution of the focused interfaces, which contained the interfaces of L1 pentamers and mAbs investigated here. The resolution of each structure was determined by gold-standard Fourier shell correlation (threshold = 0.143). Local resolution variations were evaluated by ResMap software[34]. All dataset processing is depicted in Supplementary Fig. 3 and summarized in Supplementary Table 3.

Model fitting and refinement

Atomic models of Fabs were generated via homology modeling using SWISS-MODEL[35]. Then, initial template models were generated by docking the homology Fab models and the HPV16 L1 pentamer structure (PDB code: 2R5H) into the cryo-EM densities of the final L1-Fab-complexes described above using Chimera software[36], followed by manual adjustment and correction according to protein sequences and densities in Coot software[37], as well as real space refinement using Phenix software[38]. Details of the refinement statistics of the complexes are provided in Supplementary Table 3. The footprints of Fabs were generated on a two-dimensional projection of the stereographic sphere using RIVEM software[39]. Structural figures were illustrated with ChimeraX software[40].

In vivo potency and in vitro potency assay

The quadrivalent HPV vaccine adsorbed on aluminum adjuvant, Gardasil that was provided by MERCK, produced in the yeast expression system, was incubated at 56 °C for 0, 1, 6, and 12 h (designated groups 1–4, respectively), and subjected to different degrees of heat-accelerated destruction. In the in vivo potency assay, the disrupted quadrivalent HPV vaccine was diluted to 4 μg/ml or 1.33 μg/ml, and specific-pathogen-free female BALB/c mice (6–8 weeks old) were intraperitoneally immunized (0.5 ml/mouse, eight mice/group). Four weeks after immunization, blood was collected from the inner canthus of the eye (approximately 7–8 drops of blood/mouse) and placed in a sterilized 1.5-ml centrifuge tube. After blood collection, cervical dislocation was used to euthanize the mice (The protocol was approved by the Ethics Committee of National Institutes for Food and Drug Control and the ethical approval number was No. 2023 (b) 071). Mouse blood was equilibrated at room temperature for 1–2 h, then centrifuged at 6000 rpm for 10 min. The serum was aseptically separated, and the ID_{50} of the serum was detected using the above PBNA method. In vitro potency assay was performed by first coating 96-well microplate with the mAb diluted in phosphate-buffered saline at a concentration of 2 μg/ml. The disrupted quadrivalent HPV vaccine were unadsorbed with citrate and then prepared in 0.5% BSA-PBST at 8 concentrations of 4.6,13.7, 41, 123, 370, 1111, 3333, and 10,000 ng/mL, and 100 μL of each dilution was added to the assay plate. The plate was allowed to incubate for 1 h at 37 °C and was washed before 100 μL of the diluted HRP-mAb at a concentration of 2 μg/mL was added. All loaded plates were subsequently incubated at 37 °C for 1 h, washed three times with PBST, and developed with TMB. The reaction was stopped with 2 N H_2SO4 and the optical density (OD) of each well of the plate was determined on a microplate reader at 450/620 nm.

Data availability

Data supporting the findings of this study are available from the corresponding author upon reasonable request. The cryo-EM density maps and corresponding atomic models have been deposited in the Electron Microscopy Data Bank (EMDB, http://www.ebi.ac.uk/pdbe/emdb/) and Protein Bank (PDB, https://www.ebi.ac.uk/pdbe/), respectively. The accession codes are: HPV6 L1 pentamer in complex with Fab 6-F5-77 (EMDB: EMD-39193, PDB: 8YEF), HPV11 L1 pentamer in complex with Fab 11-F5-187 (EMDB: EMD-39194, PDB: 8YEG), HPV16 L1 pentamer in complex with Fab 16-F5-196 (EMDB: EMD-39195, PDB: 8YEH), and HPV18 L1 pentamer in complex with Fab 18-F5-203 (EMDB: EMD-39196, PDB: 8YEI).

Received: 17 March 2024; Accepted: 11 March 2025;
Published online: 22 March 2025

References

1. Sung, H. et al. Global Cancer Statistics 2020: GLOBOCAN Estimates of Incidence and Mortality Worldwide for 36 Cancers in 185 Countries. *CA Cancer J. Clin.* **71**, 209–249 (2021).
2. Durst, M., Gissmann, L., Ikenberg, H. & zur Hausen, H. A papillomavirus DNA from a cervical carcinoma and its prevalence in cancer biopsy samples from different geographic regions. *Proc. Natl Acad. Sci. USA* **80**, 3812–3815 (1983).
3. Zur Hausen, H. Papillomaviruses and cancer: from basic studies to clinical application. *Nat. Rev. Cancer* **2**, 342–350 (2002).
4. Group, F. I. S. Quadrivalent vaccine against human papillomavirus to prevent high-grade cervical lesions. *N. Engl. J. Med.* **356**, 1915–1927 (2007).
5. De Martel, C., Plummer, M., Vignat, J. & Franceschi, S. Worldwide burden of cancer attributable to HPV by site, country and HPV type. *Int. J. Cancer* **141**, 664–670 (2017).
6. Malvolti, S. et al. The Global Demand and Supply Balance of the Human Papillomavirus Vaccine: Implications for the Global Strategy for the Elimination of Cervical Cancer. *Vaccines* **12**, https://doi.org/10.3390/vaccines12010004 (2023).
7. *WHO Expert Committee on Biological Standardization*. World Health Organ Tech Rep Ser Sixty-first report, 1-267 (WHO, 2016).
8. Shank-Retzlaff, M. et al. Correlation between mouse potency and in vitro relative potency for human papillomavirus Type 16 virus-like particles and Gardasil vaccine samples. *Hum. Vaccin* **1**, 191–197 (2005).
9. Uhlrich, S., Coppens, E., Moysan, F., Nelson, S. & Nougarede, N. In *Alternatives to Animal Testing* Ch. 10, 76–82 (Springer, Singapore, 2019).
10. Metz, B., Hendriksen, C. F., Jiskoot, W. & Kersten, G. F. Reduction of animal use in human vaccine quality control: opportunities and problems. *Vaccine* **20**, 2411–2430 (2002).
11. Huang, W. et al. Structural characterization of a neutralizing mAb H16.001, a potent candidate for a common potency assay for various HPV16 VLPs. *NPJ Vaccines* **5**, 89 (2020).
12. Roberts, C. et al. Development of a human papillomavirus competitive luminex immunoassay for 9 HPV types. *Hum. Vaccin Immunother.* **10**, 2168–2174 (2014).
13. Liu, X. et al. Neutralization sites of human papillomavirus-6 relate to virus attachment and entry phase in viral infection. *Emerg. Microbes Infect.* **8**, 1721–1733 (2019).
14. He, M. et al. Structural basis for the shared neutralization mechanism of three classes of human papillomavirus type 58 antibodies with disparate modes of binding. *J. Virol.* **95**, https://doi.org/10.1128/JVI.01587-20 (2021).
15. Richards, K. F., Bienkowska-Haba, M., Dasgupta, J., Chen, X. S. & Sapp, M. Multiple heparan sulfate binding site engagements are required for the infectious entry of human papillomavirus type 16. *J. Virol.* **87**, 11426–11437 (2013).
16. Buck, C. B. et al. Arrangement of L2 within the papillomavirus capsid. *J. Virol.* **82**, 5190–5197 (2008).
17. Day, P. M. & Schiller, J. T. The role of furin in papillomavirus infection. *Fut. Microbiol.* **4**, 1255–1262 (2009).
18. Leder, C., Kleinschmidt, J. A., Wiethe, C. & Muller, M. Enhancement of capsid gene expression: preparing the human papillomavirus type 16

major structural gene L1 for DNA vaccination purposes. *J. Virol.* **75**, 9201–9209 (2001).
19. Pastrana, D. V. et al. Reactivity of human sera in a sensitive, high-throughput pseudovirus-based papillomavirus neutralization assay for HPV16 and HPV18. *Virology* **321**, 205–216 (2004).
20. Pastrana, D. V. et al. Cross-neutralization of cutaneous and mucosal Papillomavirus types with anti-sera to the amino terminus of L2. *Virology* **337**, 365–372 (2005).
21. Mossadegh, N. et al. Codon optimization of the human papillomavirus 11 (HPV 11) L1 gene leads to increased gene expression and formation of virus-like particles in mammalian epithelial cells. *Virology* **326**, 57–66 (2004).
22. Johnson, K. M. et al. Role of heparan sulfate in attachment to and infection of the murine female genital tract by human papillomavirus. *J. Virol.* **83**, 2067–2074 (2009).
23. Smith, K. et al. Rapid generation of fully human monoclonal antibodies specific to a vaccinating antigen. *Nat. Protoc.* **4**, 372–384 (2009).
24. Brown, M. J., Seitz, H., Towne, V., Muller, M. & Finnefrock, A. C. Development of neutralizing monoclonal antibodies for oncogenic human papillomavirus types 31, 33, 45, 52, and 58. *Clin. Vaccin. Immunol.* **21**, 587–593 (2014).
25. Wu, X. L., Zhang, C. T., Zhu, X. K. & Wang, Y. C. Detection of HPV types and neutralizing antibodies in women with genital warts in Tianjin City, China. *Virol. Sin.* **25**, 8–17 (2010).
26. Nie, J., Liu, Y., Huang, W. & Wang, Y. Development of a Triple-Color Pseudovirion-Based Assay to Detect Neutralizing Antibodies against Human Papillomavirus. *Viruses* **8**, 107 (2016).
27. Nie, J., Huang, W., Wu, X. & Wang, Y. Optimization and validation of a high throughput method for detecting neutralizing antibodies against human papillomavirus (HPV) based on pseudovirons. *J. Med. Virol.* **86**, 1542–1555 (2014).
28. Matumoto, M. A note on some points of calculation method of LD50 by Reed and Muench. *Jpn. J. Exp. Med.* **20**, 175–179 (1949).
29. Opalka, D. et al. Simultaneous quantitation of antibodies to neutralizing epitopes on virus-like particles for human papillomavirus types 6, 11, 16, and 18 by a multiplexed luminex assay. *Clin. Diagn. Lab. Immunol.* **10**, 108–115 (2003).
30. Nolan, K. M. et al. Development and Validation of Two Optimized Multiplexed Serologic Assays for the 9-Valent Human Papillomavirus Vaccine Types. *mSphere* **8**, e0096221 (2023).
31. Zivanov, J. et al. New tools for automated high-resolution cryo-EM structure determination in RELION-3. *Elife* **7**, https://doi.org/10.7554/eLife.42166 (2018).
32. Zhang, K. Gctf: Real-time CTF determination and correction. *J. Struct. Biol.* **193**, 1–12 (2016).
33. Punjani, A., Rubinstein, J. L., Fleet, D. J. & Brubaker, M. A. cryoSPARC: algorithms for rapid unsupervised cryo-EM structure determination. *Nat. Methods* **14**, 290–296 (2017).
34. Kucukelbir, A., Sigworth, F. J. & Tagare, H. D. Quantifying the local resolution of cryo-EM density maps. *Nat. Methods* **11**, 63–65 (2014).
35. Waterhouse, A. et al. SWISS-MODEL: homology modelling of protein structures and complexes. *Nucleic Acids Res.* **46**, W296–W303 (2018).
36. Pettersen, E. F. et al. UCSF Chimera-a visualization system for exploratory research and analysis. *J. Comput Chem.* **25**, 1605–1612 (2004).
37. Emsley, P. & Cowtan, K. Coot: model-building tools for molecular graphics. *Acta Crystallogr. D. Biol. Crystallogr.* **60**, 2126–2132 (2004).
38. Adams, P. D. et al. PHENIX: a comprehensive Python-based system for macromolecular structure solution. *Acta Crystallogr. D. Biol. Crystallogr.* **66**, 213–221 (2010).
39. Xiao, C. & Rossmann, M. G. Interpretation of electron density with stereographic roadmap projections. *J. Struct. Biol.* **158**, 182–187 (2007).
40. Goddard, T. D. et al. UCSF ChimeraX: Meeting modern challenges in visualization and analysis. *Protein Sci.* **27**, 14–25 (2018).

Acknowledgements

We would like to thank Dr. John T. Schiller for providing the plasmids encoding the structural genes (L1 and L2). Work was supported by Ministry of Science and Technology of China (CPL-1233 and SRPG22-003), National Key Research and Development Program (2018YFA0900801), CAS (YSBR-010) and the National Science Foundation Grants (12034006, 32325004 and T2394482). Xiangxi Wang was supported by National Science Fund for Distinguished Young Scholar (No. 32325004) and the NSFS Innovative Research Group (No. 81921005).

Author contributions

N.X, X.W. and W.H. designed, planned the work, and revised the manuscript. J.H. and Z.J. performed the experiment, analyzed the data, and drafted the manuscript. M.W., Q.Z., H.Q, and J.N. partially performed the PBNA experiments. L.N., X.X, L.X. and F.W. partially performed the ELISA experiments. W.F. and S.L. partially performed the cryo-EM structure analysis. Y.C., B.X., T.L., and D.L. partially performed the animal experiments. All authors read and approved the final manuscript.

Competing interests

The authors declare no competing interests.

Additional information

Supplementary information The online version contains supplementary material available at https://doi.org/10.1038/s41541-025-01106-z.

Correspondence and requests for materials should be addressed to Ningshao Xia, Xiangxi Wang or Weijin Huang.